Coupling and tuning of modal frequencies in direct current biased microelectromechanical systems arrays

Prashant N. Kambali,[1] Gyanadutta Swain,[1] Ashok Kumar Pandey,[1,a)] Eyal Buks,[2] and Oded Gottlieb[3]

[1]*Department of Mechanical and Aerospace Engineering, IIT Hyderabad, Yeddumailaram 502205, India*
[2]*Faculty of Electrical Engineering, Technion-Israel Institute of Technology, Haifa 32000, Israel*
[3]*Faculty of Mechanical Engineering, Technion-Israel Institute of Technology, Haifa 32000, Israel*

Understanding the coupling of different modal frequencies and their tuning mechanisms has become essential to design multi-frequency MEMS devices. In this work, we fabricate a MEMS beam with fixed boundaries separated from two side electrodes and a bottom electrode. Subsequently, we perform experiments to obtain the frequency variation of in-plane and out-of-plane mechanical modes of the microbeam with respect to both DC bias and laser heating. We show that the frequencies of the two modes coincide at a certain DC bias, which in turn can also be varied due to temperature. Subsequently, we develop a theoretical model to predict the variation of the two modes and their coupling due to a variable gap between the microbeam and electrodes, initial tension, and fringing field coefficients. Finally, we discuss the influence of frequency tuning parameters in arrays of 3, 33, and 40 microbeams, respectively. It is also found that the frequency bandwidth of a microbeam array can be increased to as high as 25 kHz for a 40 microbeam array with a DC bias of 80 V. © 2015 AIP Publishing LLC. [http://dx.doi.org/10.1063/1.4928536]

Sensitivity of resonant sensors and actuators based on a single element of micro or nanobeam can be improved by increasing the resonance frequency and quality factor of the system.[1–5] However, due to the process of increasing quality factor, the frequency bandwidth of the device reduces as it is inversely proportional to the quality factor. Consequently, recent studies reveal that micro- or nanoelectromechanical system (MEMS/NEMS) based array has been used to increase the frequency bandwidth using various frequency tuning mechanisms without any major shift in its sensitivity.[6–10] Afterwards, there were several theoretical studies concerning the coupled behavior of array dynamics.[9,11] Krylov et al.[9] discussed the coupling of out-of-plane modes in a cantilever array under parametric excitation due to electrostatic fringing forces. Thijssen et al.[10] demonstrated the driven parametric amplification of in-plane motion of an array of nanobeams with varying width excited due to photothermal effects. All the above studies are either limited to an in-plane mode or an out-of-plane mode. In this letter, we discuss about the frequency tuning and coupling of in-plane and out-of-plane modes of fixed-fixed beam arrays as shown in Fig. 1 due to DC bias under the electrostatic direct as well as fringing field effects. Additionally, we separate the frequencies of beams by varying the initial tension of the beams due to photothermal effects. Finally, we present a theoretical model to analyse the effect of different frequency tuning parameters such as the air-gap thickness between the beams, the fringing field effects, etc.

To demonstrate the frequency tuning of two mechanical modes due to DC bias of a single beam and a multibeam array, we fabricate a single clamped-clamped beam separated by two side electrodes, and also an array of three

beams, 33 beams (not shown), and 40 beams, as shown in Figs. 1(a)–1(c). All the beams are made of AuPd alloy on a silicon substrate using the bulk micromachining process.[3,7] The fabricated beams are of the same dimensions with length $L = 500\,\mu m$, width $B = 4\,\mu m$, and height $H = 200\,nm$. Each beam is separated from its adjacent neighbors by different gaps ranging from $1\,\mu m$ to $7\,\mu m$ and also from the bottom substrate by a gap of $d = 500\,\mu m$.

To experimentally characterize the system of single as well as an array of multibeams, we use a laser based detection technique[3] as shown in Fig. 1(d). To obtain the variation of two mechanical modes (corresponding to in-plane and out-of-plane) of a single beam in its linear range, we apply a combined signal of DC and AC voltage to the beam and ground the side electrodes and bottom electrode, respectively. To measure the response, we use a laser power of 15.9 mW. On increasing the DC voltage from 0 to 90 V and keeping low AC voltage (1–40 mV) to get the linear response, we find that the frequency corresponding to an in-plane mode decreases due to the well-known electrostatic softening effect[3,7] and that an out-of-plane frequency increases due to the stretching of the beam in the in-plane direction,[3] as shown in Fig. 2(a). Consequently, we obtain a crossing point of equal in-plane and out-of-plane frequencies at a DC voltage of 81 V. To investigate the effect of laser heating on the value of the frequency at crossing point F_s corresponding to DC voltage V_s, and the frequencies of two mechanical modes, F_1 and F_2, at zero DC voltage, we vary laser power, L_p, from 0.06 to 20 mW. We found that as L_p varies from 0.06 to 20 mW, the frequencies F_1 and F_2 reduce individually. However, we noticed that the difference $\Delta F = F_2 - F_1$ increases from 7.5 kHz to 7.8 kHz due to heating. We also found that the crossing point lowers from 90 V to 80 V as laser power varies from 0.06 to 20 mW. Such
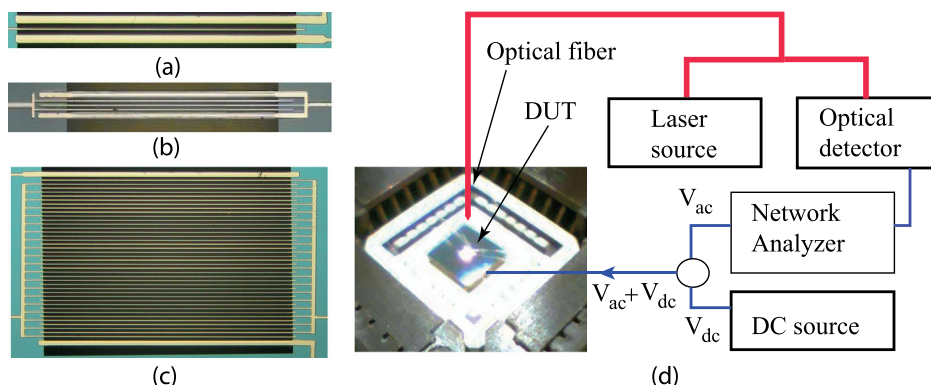
FIG. 1. An arrangement of single and multibeams arrays with side electrodes and a bottom electrode are shown with: (a) a single beam element, (b) three beam elements, and (c) 40 beam elements. (d) An outline of optical based characterization setup to characterize single as well as multibeams arrays.

variation indicates to a high sensitivity of the beam with respect to the temperature due to differential thermal expansion of beam and the substrate.[3]

After showing the frequency variation of two mechanical modes and the frequency crossing of a single beam, we investigate the frequency tuning in a three beam array. Figure 2(c) shows frequency variation of in-plane and out-of-plane modes when the optical fiber with a fixed laser power is moved across the width of the three beam array due to localized heating of different beams. Figure 2(d) shows the frequency and DC voltage relation of the three beam array system with different DC voltages when the optical fiber is fixed at around $22\,\mu m$ from the side electrode, as shown in the Fig. 2(c). Unlike the single beam, we also observe frequency crossings between the modes of

adjacent beams and those of non-adjacent beams. Here, the latter frequency crossing is defined as a point when the two crossing modes do not show any coupling. Such points are observed when the modal frequencies of non-adjacent beams coincide with each other. We also noticed that the coupling strength of the modes of side beams is very low as compared to that of the middle beam, probably due to a non-uniform gap between the middle beam and the two side beams.

Finally, we perform experiments with arrays of 33 and 40 beams, respectively, by locating the optical fiber with fixed laser power at the middle of each array. Consequently, we find that the frequencies of two mechanical modes of each beam corresponding to zero DC voltage are distributed over $5\,kHz$ due to non-uniform heating of
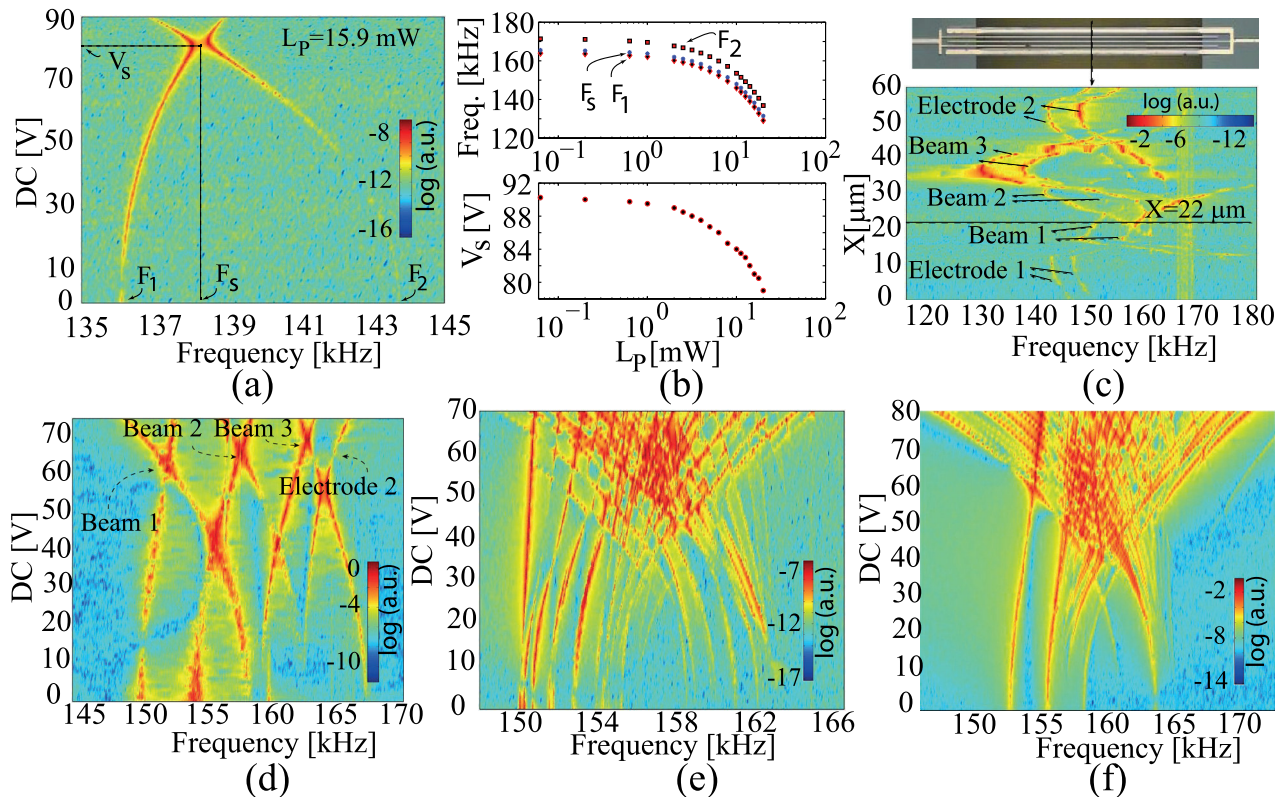

FIG. 2. (a) Experimental results showing the variation of out-of-plane and in-plane frequencies of a single beam separated by two side electrodes with DC bias, where F_1 and F_2 are out-of-plane and in-plane frequencies at $V_{dc} = 0$, F_s and V_s are frequency and corresponding DC voltage at avoided crossing point when the laser power is fixed at $L_p = 15.9$ mW. (b) Variation of F_1, F_2, F_s, and V_s with laser power L_p [mW]. (c) Variation of the frequencies of three beams array due to change in the position of optical fiber with a fixed laser power and fixed excitation. (d) Frequency response of three beam arrays with DC bias when the position of optical fiber is fixed at around $X = 22\,\mu m$. Frequency response of an array of (e) 33 beams and (f) 40 beams vs. DC bias. (Color plots in all the figures show logarithmic value of the network analyzer signal in arbitrary unit.)

the beams in arrays of 33 and 40 beam, as shown in Figs. 2(e) and 2(f), respectively. On increasing the DC voltage from 0 to 70 V for the 33 beam array and 0 to 80 V for the 40 beam array, we obtain the similar variation of the in-plane and out-of-plane modes as for the case of single and three beam systems. However, unlike the single beam, the modal frequencies of multibeam array are found to be uniform over a large range of frequencies when the DC bias is increased beyond that of the equal frequency crossings. Such a uniform distribution becomes closely spaced as the number of elements in an array increases. For example, the frequency bandwidth of the closely spaced response of a 40 beam array increases from 15 kHz to 25 kHz when the DC voltage increases from 60 to 80 V. Since the quality factor of each beam is around 10^4 and its modal frequency is in the range of 150–160 kHz, the bandwidth of a single beam system can be approximated in the range of 15–16 Hz. On the other hand, by tuning the modal frequencies of a 40 beam array, a bandwidth of 25 kHz can be obtained at DC voltage of 80 V. Further study is needed in order to investigate the feasibility of exploiting the enhanced bandwidth for improving performance of sensors based on coupled arrays of mechanical resonators. In the following paragraph, we present a brief theoretical analysis to show the effect of the gap on the frequency crossing values of in-plane and out-of-plane modes of a single beam as well as beams in different array configurations.

To demonstrate the influence of side electrodes on the coupling region, we develop a theoretical model for an array of N clamped-clamped beams having length L, width B, and thickness H, as shown in Fig. 3(a), where E_1 and E_2 are two fixed side electrodes, and E_g is the fixed bottom electrode. The beams are separated from their neighboring beams by different gaps g_0, g_1, g_2,…, g_N and also from the bottom electrode by a distance d. To develop a consistent dynamical model, let us consider n^{th} beam separated from $(n-1)^{th}$ and $(n+1)^{th}$ beams by the gaps g_{n-1} and g_{n+1} and also from the bottom electrode by a distance d as shown in Fig. 3(b), where $\bar{y}_n$ and $\bar{z}_n$ are the deflections in the in-plane and out-of-plane directions, respectively. It is also assumed that the in-plane and transverse oscillations of the beam are achieved under

the influence of direct and fringing field forces[12] which are captured by Q_{ny} and Q_{nz}, as shown in Fig. 3(c). Finally, the governing equations of motion in the $\bar{y}$ and $\bar{z}$ directions of nth beam, including the residual tension and mid-plane stretching,[5] can be written as

$$EI_{\bar{z}}\bar{y}_n'''' + \rho A \ddot{\bar{y}}_n - \left[N_{n0} + \frac{EA}{2L}\int_0^L (\bar{z}_n'^2 + \bar{y}_n'^2)d\bar{x}_n\right]\bar{y}_n''$$
$$= Q_{n\bar{y}}(\bar{y}, \bar{z}, \bar{t}),$$

$$EI_{\bar{y}}\bar{z}_n'''' + \rho A \ddot{\bar{z}}_n - \left[N_{n0} + \frac{EA}{2L}\int_0^L (\bar{z}_n'^2 + \bar{y}_n'^2)d\bar{x}_n\right]\bar{z}_n''$$
$$= Q_{n\bar{z}}(\bar{y}, \bar{z}, \bar{t}),$$

where $'$ and $\cdot$ represent differentiation w.r.t. $\bar{x}$ and $\bar{t}$, respectively, $n = 1, 2,…, N$. N_{n0} is the initial tension induced due to residual stresses[5] and heating,[3] etc., $EI_{\bar{y}}$ and $EI_{\bar{z}}$ are the flexural rigidity components of $\bar{y}$ and $\bar{z}$, respectively, and $I_{\bar{y}} = BH^3/12$ and $I_{\bar{z}} = HB^3/12$ are moments of inertia. E is the Young's modulus, and ρ is the material density. The expressions for electrostatic forcing Q_{ny} and Q_{nz} per unit length of nth beam along $\bar{y}$ and $\bar{z}$ directions include the effect of direct and fringing field[9,12,13] based on numerical simulation in COMSOL multiphysics software as described in the supplementary information.[14] In the forcing expression of Q_{ny} and Q_{nz}, we also define k_1 to capture the net effect of fringing and direct fields in $\bar{y}$-direction, k_2 to capture the fringing field effects due to extended bottom electrode,[13] and k_3 to capture the effectiveness of parametric fringing field effect due to side beams when the beam is subjected to a deflection of $\bar{z}(t)$,[12] $V_{i,j} = V_i - V_j$ is the difference in the DC voltage applied between i^{th} and j^{th} elements.

To obtain the modal dynamic equations, we approximate the displacements by the single mode shape, which satisfies the undamped and unforced linear boundary-value problem exactly. The total displacement along y and z-directions consist of the static displacements due to DC voltage and dynamic displacement due to AC voltage.[15] After substituting the assumed solution and then applying Galerkin's method, the modal dynamic equation corresponding to an in-plane mode, i, and an
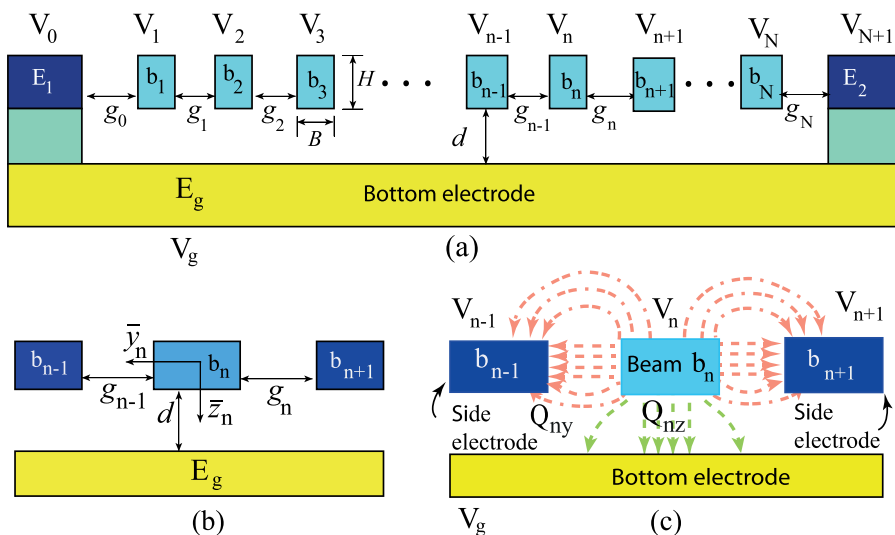

FIG. 3. (a) Side view of N fixed-fixed beams and the side electrodes, E_1 and E_2, and the ground electrode E_g. (b) Displacement of the beam in two different directions are represented by y and z. (c) The corresponding forces are represented by Q_z and Q_y. (Geometric parameters are also mentioned at appropriate location.)

out-of-plane mode, o, of N beams can be written in the matrix form, $\ddot{P} + [M]P = 0$,[5] where P is the state variables given by $[P] = [P_{11}\ P_{12}\ \ldots\ P_{k1}\ P_{k2}\ \ldots\ P_{N1}\ P_{N2}]^{T}$ and M, respectively. The matrix M contains terms for uncoupled modal frequencies of N beams corresponding to i and o modes, respectively. It also contains modal coupling of the frequencies of adjacent beams. Finally, the frequencies corresponding to the modes of each beam of an array can be found by taking the square root of the eigenvalues of matrix $[M]$. Consequently, for N beams, there are $2N$ modes. The frequencies of $2N$ modes of an array of N beams can be tuned using different initial tension N_0 and DC bias V. A detailed derivation of the reduced-order form and definition of related terms are found in the supplementary information.[14]

To demonstrate the importance of different frequency tuning parameters, we first find the physical properties E, ρ, and the initial tension N by comparing the analytical and experimental results for a single as well as multibeams arrays. In the case of the single beam arrangement, the side beams are fixed; therefore, there exists the coupling between i and o modes of the single beam. Hence, the size of P and M for $N = 1$ reduce to 2×1 and 2×2, where λ_{11}, λ_{12}, c_{1io}, and c_{1oi} are the only non-zero terms in matrix M as defined in Ref. 14. By comparing the outcome of the analytical model with experimental results, we get $E = 2.58 \times 10^{10}\,\mathrm{N/m^2}$, $\rho = 3227.4\,\mathrm{kg/m^3}$, and $N_0 = 38.3\,\mu\mathrm{N/m}$ corresponding to the gaps of $g_0 = 4.5\,\mu\mathrm{m}$ and $g_1 = 7\,\mu\mathrm{m}$ and the forcing coefficients $k_1 = 0.945$, $k_2 = 2.6$, and $k_3 = 1.3$. Figure 4(a) shows the comparison of analytical and experimental results with the frequency crossing depicted in Fig. 2(a). We found that when the gaps between the beam and the side electrodes/fixed beams are the same, the frequency crossing disappears. We also noticed that the frequency crossing can be tuned by parametric fringing forces from the side electrodes in z-direction. While the fringing forces from the bottom

electrode (located at around $500\,\mu\mathrm{m}$) plays a little role in controlling the out-of-plane response, the effect of direct forces is found to be insignificant. Similarly, we compute the frequency tuning in an array of three beams, 33 beams, and 40 beams, respectively. For the three beam array, we take $N = 3$ in which three in-plane and out-of-plane modes can be tuned with initial tension, gap thickness, fringing forces, etc. On comparing the results with experiments, we obtain the physical parameters as $E = 3.183 \times 10^{10}\,\mathrm{N/m^2}$, $\rho = 3234.2\,\mathrm{kg/m^3}$, and $N_0 = 46.86\,\mu\mathrm{N/m}$, as shown in Figure 4(b). The frequencies of i and o modes of three different beams are obtained by first tuning the initial tensions $N_1 = N_0$, $N_2 = 1.06N_0$, and $N_3 = 1.13N_0$ corresponding to zero DC voltage, then the fringing field parameters $k_1 = 0.35$, 0.40, 0.40, $k_2 = 1$, 1, 1, and $k_3 = 1.8$, 2.7, 2.5 for the three beams having the air-gaps of $g_0 = 2\,\mu\mathrm{m}$, $g_1 = 2.7\,\mu\mathrm{m}$, $g_2 = 4.9\,\mu\mathrm{m}$, and $g_3 = 4.5\,\mu\mathrm{m}$, respectively. Similarly, we also obtain the analytical variation of frequencies of arrays of 33 and 40 beams, as shown in Figs. 4(c) and 4(d), respectively, which are similar to the experimentally obtained curves, as shown in Figs. 2(e) and 2(f). For both arrays, we use the same physical properties as that of the three beams array, but the initial tensions of the beams vary from N_0 to $1.065N_0$ for $N = 33$, and $1.0525N_0$ to $1.11N_0$ for $N = 40$ to fit the frequencies at a zero DC voltage. To obtain the variation at a non-zero DC voltage in both cases, the gaps, g_i, $i = 0$, 1, …, N, are taken in the range of $1\,\mu\mathrm{m}$–$5\,\mu\mathrm{m}$, and the fringing force coefficients k_1 varies from 0 to 2.98, $k_2 = 1$, and $k_3 = 2.5$ for all beams. By varying the gap and forcing coefficients, we found that the strength of several frequency crossings of inter- and intramodal coupling of same or different beams can be obtained. A future application of the equal crossing frequencies may serve as necessary conditions for internal resonances and as such may contribute to multi-functional sensing.[16,17] The nonlinear vibration properties of the arrays can also be explored to get the locked
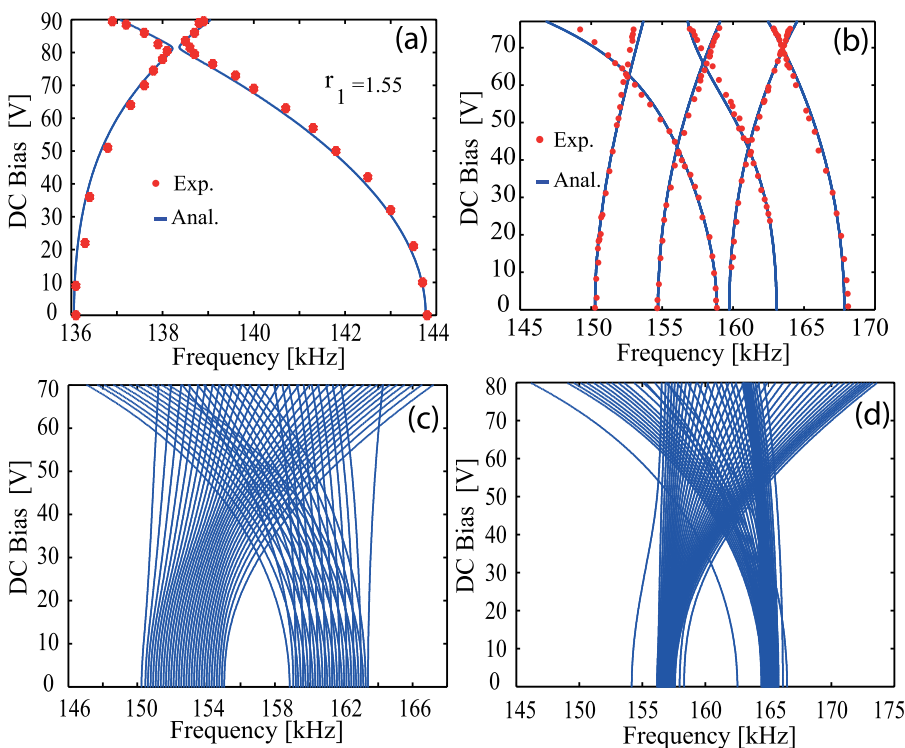

FIG. 4. Comparison of experimental and analytical results for (a) single beam with gap ratios $r_0 = 1$ and $r_1 = 1.55$ and (b) three beam arrays with gap ratios $r_0 = 1$, $r_1 = 1.35$, $r_2 = 2.45$, and $r_3 = 2.25$. Analytical results showing the variation of frequencies vs DC voltage for arrays of (c) 33 beams and (d) 44 beams, respectively. Here, $r_n = \frac{g_n}{g_0}$, $n = 0, \ldots, N$.

modes.[18] Additionally, we found that by varying the initial tensions of different beams, we can significantly increase the bandwidth of a multibeam array system.

In conclusion, we have performed a combined experimental and theoretical investigation to show that the frequency tuning of DC biased single beam and arrays of multiple beams due to various parameters such as initial tension, air-gap thickness, and fringing field effects. We have also shown that the inter- and intramodal coupling can be controlled by the air-gap thickness as well as fringing field effects. Possible discrepancies between linear theory and the array experiments can be explained by effects of nonlinearities such as resonance frequency dependence on the response amplitude [11] and nonlinear damping[19] neglected in this study.

[1] S. S. Verbridge, D. F. Shapiro, H. G. Craighead, and J. M. Parpia, Nano Lett. **7**(6), 1728 (2007).

[2] A. K. Pandey and R. Pratap, J. Micromech. Microeng. **17**(12), 2475 (2007).

[3] A. K. Pandey, O. Gottlieb, O. Shtempluck, and E. Buks, Appl. Phys. Lett. **96**, 203105 (2010).

[4] I. Kozinsky, H. W. Ch. Postma, I. Bargatin, and M. L. Roukes, Appl. Phys. Lett. **88**, 253101 (2006).

[5] A. K. Pandey, J. Micromech. Microeng. **23**(8), 085015-1–085015-10 (2013).

[6] M. Spletzer, A. Raman, H. Sumali, and J. P. Sullivan, Appl. Phys. Lett. **92**, 0114102 (2008).

[7] E. Buks and M. L. Roukes, J. Microelectromech. Syst. **11**(6), 802 (2002).

[8] M. K. Zalalutdinov, J. W. Baldwin, M. H. Marcus, R. B. Reichenbach, J. M. Parpia, and B. H. Houston, Appl. Phys. Lett. **88**, 143504 (2006).

[9] S. Krylov, S. Lulinsky, B. R. Ilic, and I. Schneider, Appl. Phys. Lett. **105**, 071909 (2014).

[10] R. Thijssen, T. J. Kippenberg, A. Polman, and E. Verhagen, ACS Photonics **1**, 1181 (2014).

[11] S. Gutschmidt and O. Gottlieb, Nonlinear Dyn. **67**, 1 (2012).

[12] P. N. Kambali and A. K. Pandey, J. Comput. Nonlinear Dyn. **10**, 051010 (2015).

[13] Q. P. Unterreithmeier, E. M. Weig, and J. P. Kotthaus, Nat. Lett. **458**, 1001 (2009).

[14] See supplementary material at http://dx.doi.org/10.1063/1.4928536 for the details of static and dynamic equations of in-plane and out-of-plane modes.

[15] A. H. Nayfeh, M. I. Younis, and E. M. Abdel-Rahman, Nonlinear Dyn. **48**, 153–163 (2007).

[16] O. Sahin, S. Magonov, C. Su, C. F. Quate, and O. Solgaard, Nat. Nanotechnol. **2**, 507 (2007).

[17] E. Hacker and O. Gottlieb, Appl. Phys. Lett. **101**, 053106 (2012).

[18] M. Sato, B. E. Hubbard, A. J. Sievers, B. Illic, D. A. Czaplewski, and H. G. Craighead, Phys. Rev. Lett. **90**(4), 044102 (2003).

[19] S. Zaitsev, O. Shtempluck, E. Buks, and O. Gottlieb, Nonlinear Dyn. **67**, 859 (2012).